

Study on Effects of Orientation on Wall Boiling Heat Flux Partitioning

Satbyoul Jung^a, Hyungdae Kim^{a*}

^a Department of Nuclear Engineering, Kyung Hee University, Republic of Korea

*Corresponding author: hdkims@khu.ac.kr

1. Introduction

Nucleate boiling is widely used in practical applications, safety system design for Light Water Reactors (LWRS), due to its highly efficient heat transport capability. It is one of the most complex phenomena that is typically modelled with correlations having some mechanistic basis and empirical data. There have been a number of efforts into development of two-phase thermal hydraulics code, especially, to investigate the boiling heat transfer phenomena with high-resolution [1-2].

Several models for wall heat flux partitioning have been proposed [3-5]. However, all the models were developed based on a horizontal wall and thus the effect of wall orientation were not considered even though the boiling heat transfer mechanisms could be strongly distorted by the effects of the wall orientation, for example, bubble sliding and merging.

In this study, the high-resolution wall boiling heat flux partitioning experiments were conducted to simultaneously gather the data of liquid-vapor phase, temperature and heat flux distributions on the wall and the bubble dynamics during saturated nucleate boiling. The focus of the study exists on the effect of wall orientation on the heat flux partitioning.

2. Heat Partitioning Model (PRI model)

The heat partitioning model, PRI model, proposed by Kurul and Podowski [3] is the most widely used in the numerical code for high-resolution two-phase thermal hydraulic analysis. The heat transferred from wall to fluid with three mechanisms by evaporation, quenching and convection as shown in Fig. 1. The total wall heat flux, q''_w is as follow:

$$q''_w = q''_e + q''_q + q''_c \quad (1)$$

Evaporation heat flux, q''_e is the latent heat flux to form the bubbles and is expressed as:

$$q''_e = N'' f \left(\frac{\pi}{6} D_d^3 \right) \rho_g h_{fg} \quad (2)$$

where N'' is the bubble nucleation site density, f is the bubble frequency, D_d is the bubble departure diameter, ρ_g is the density of gas and h_{fg} is the latent heat for evaporation.

Quenching heat flux, q''_q is the heat flux expended in re-formation of the thermal boundary layer and is expressed as:

$$q''_q = \left(\frac{2}{\sqrt{\pi}} \sqrt{t_w k_l \rho_l C_{pl} f} \right) A_{2f} (T_w - T_l) \quad (3)$$

where t_w is bubble waiting time, k_l is the conductivity of liquid, C_{pl} is the specific heat of liquid, A_{2f} is the ratio of two-phase area to total area, T_w is the wall temperature and T_l is the liquid temperature.

Convection heat flux, q''_c is the heat flux transferred to the liquid phase outside the bubble influence area and is as follow:

$$q''_c = h_c A_{1f} (T_w - T_l) \quad (4)$$

where A_{1f} the ratio of single phase area to total area.

Table I shows the correlation for bubble parameters that makes up the wall heat partitioning model. As the bubble parameters in Table I is function of the wall superheat, the partitioned heat flux (or total wall heat flux) can be calculated with wall superheat.

3. Experiment

3.1 Experimental techniques

Figure 2 shows the schematic of the optical setup to measure the liquid-vapor phases and temperature distributions on the wall and the bubble shape from the side. The wall temperature distributions could be measured using an infrared (IR) camera placed below the test sample. The sample is transparent enough to acquire thermal radiation from the film heater without considerable loss of accuracy. In addition, simultaneously the liquid-vapor phases on the wall could be detected using the total reflection (TR) technique with a high speed video (HSV) and the bubble shape from the side could be observed using another high speed video.

All cameras were temporally synchronized using a function generator. The spatial/temporal resolutions of the each data were 40 μm / 0.2 ms for the temperature data, 30 μm / 0.02 ms for the phase data and 30 μm / 0.02 ms for bubble shape. For detail on experimental techniques, refer to [6].

To consider the effect of wall orientation, in addition, the optical table for array of optics and test section was designed to be rotatable, as shown in Fig. 3.

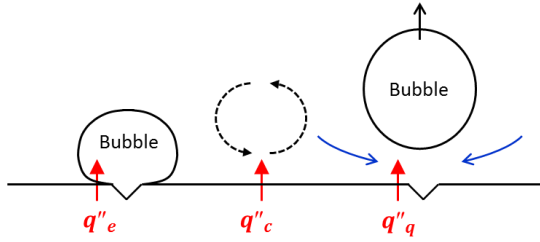


Fig. 1. Conceptual descriptions of heat flux partitioning model proposed by Kurul and Podowski [3].

Table I: Correlations of mechanistic factors in heat flux partitioning model

Factor	Correlation (CUPID 1.8)
Nucleate site density	$N'' = [185(T_w - T_{sat})]^{1.805}$
Departure frequency	$f = \sqrt{\frac{Ag(\rho_l - \rho_g)}{3D_d\rho_l}}$
Departure diameter	$D_d = 0.6 \cdot 10^{-3} e^{-\frac{T_w - T_l}{45}}$
Bubble waiting time	$t_w = \frac{0.8}{f}$
Heat transfer coefficient	$h_{c,l} = \frac{\rho_l C_{p,l} u_\tau}{T^+}$
Single phase area ratio	$A_{1f} = 1 - A_{2f}$
Two phase area ratio	$A_{2f} = N'' \frac{\pi D_b^2}{4} K$
Bubble influence factor	$K = 4$

3.2 Bubble Parameters

As the optical techniques (total reflection technique, IR thermometry technique, side visualization technique) enable the bubble parameters in the wall heat partitioning model to be measured, it is possible to directly compare the correlation for bubble parameters with the experimental results. The bubble parameters that can be measured with our experimental technique is summarized in Table II.

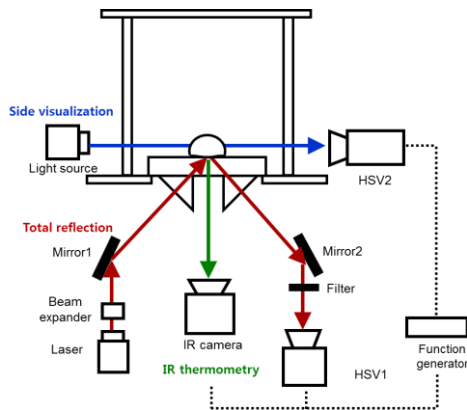


Fig. 2. Schematic of the optical system.

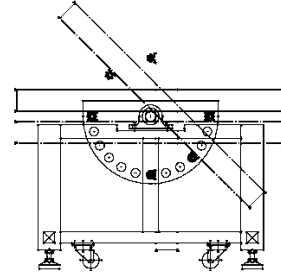


Fig. 3. Schematic of the rotatable optical table.

Table II: Bubble parameters measured using the experimental technique

Experimental techniques	Measurable bubble parameters
TR	Nucleate site density (n''), Single-phase area fraction (A_{1f}), Two-phase area fraction (A_{2f})
IR	Wall temperature (T_w)
Side view	Bubble departure diameter (D_d), Bubble frequency (f)

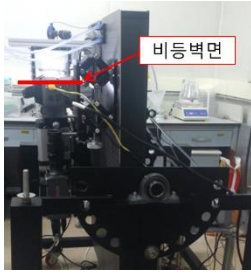
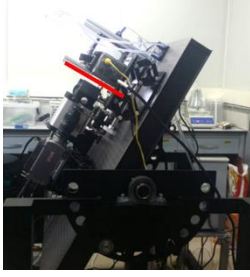
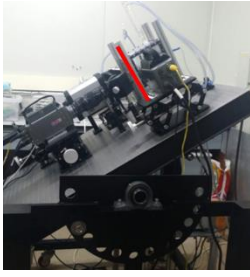

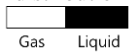
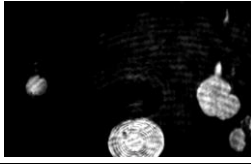

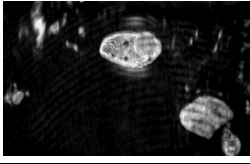
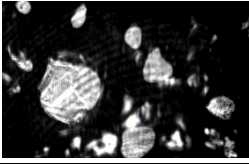

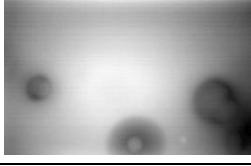
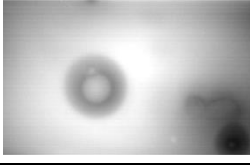
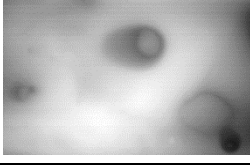
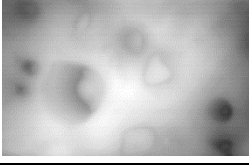

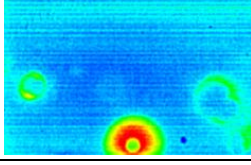
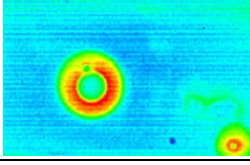
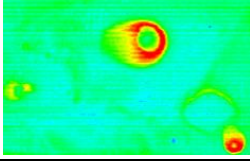
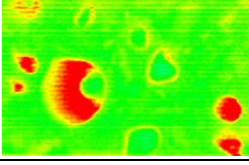
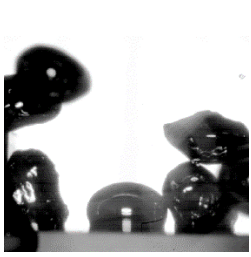
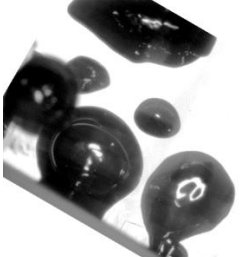
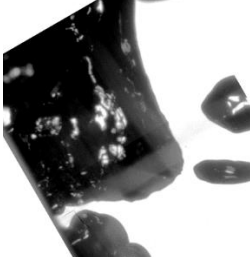

4. Results and Discussion

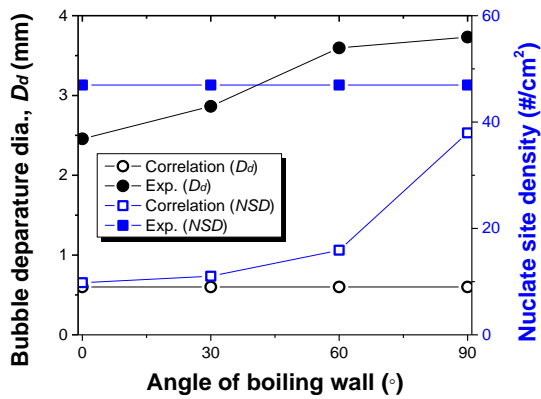
Temporally and spatially synchronized measurement data for bubble dynamics liquid-vapor phases, temperature and heat flux distribution with various wall orientation of 0° (horizontal), 30° , 60° , 90° (vertical) are presented in Table III. All the data were obtained for nucleate boiling of saturated water at $T_w=107.5^\circ\text{C}$ under atmospheric pressure. The applied heat flux to maintain the same average wall superheat were noticeably varied corresponding to the wall orientation: the applied heat flux were 202 kW/m^2 for the wall orientation of 0° , 250 kW/m^2 for 30° , 386 kW/m^2 for 60° , and 600 kW/m^2 for 90° . It is supposed that some different heat transfer mechanisms which are not incorporated in the existing heat flux partitioning model, such as bubble sliding and merging, plays a role on the inclined and vertical walls.

The experimental bubble parameters data obtained for each wall orientation were compared with the predicted values by the correlations of bubble parameters in the existing heat flux partitioning model. The comparison results are presented in Fig. 4. There are all the difference between the experimental results and the correlation data. Hence, the total wall heat flux calculated with the existing heat flux partition correlation was quite different from the experimental value, as shown in Fig. 5. In addition, it was found that the prediction error of the total wall heat flux increases as the boiling wall inclines from the horizontal to the vertical. The reason is that the existing wall boiling heat flux partitioning model was developed for the horizontal surface. The heat flux prediction error (e) was defined as,

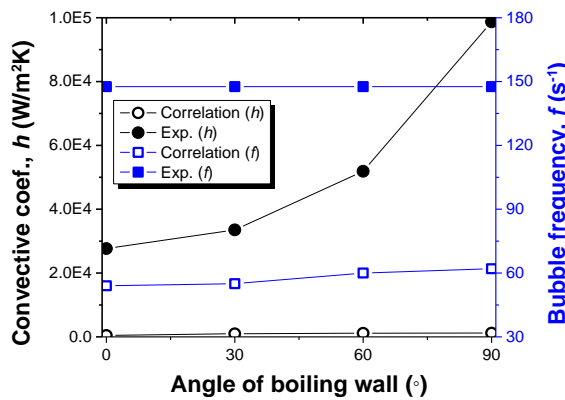
$$e = \left| \frac{q''_{\text{experiment}} - q''_{\text{prediction}}}{q''_{\text{experiment}}} \right|. \quad (5)$$

Table III: Experiment results corresponding liquid-vapor phase, temperature, and heat flux distributions on the wall and bubble shape with the wall orientation (0° , 30° , 60° , 90°) at the wall superheat of 7.5°C

Wall superheat	7.5°C			
	Applied heat flux	202 kW/m ²	250 kW/m ²	386 kW/m ²
Orientation	0°	30°	60°	90°
Experimental setup				
Phase distribution 				
Temperature distribution 				
Heat flux distribution 				
Bubble shape				



(a)



(b)

Fig. 4. Comparison of bubble parameters between experiment and correlation with various wall orientation

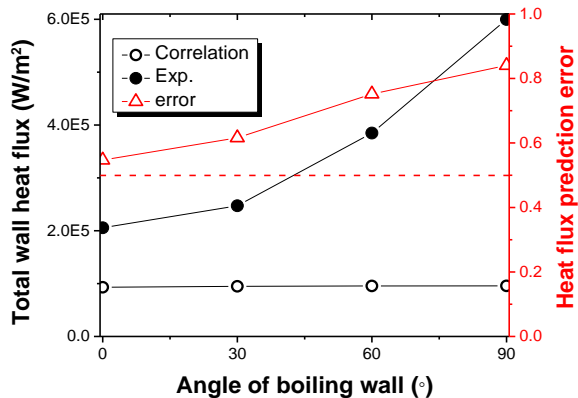


Fig. 5. Comparison of total wall heat flux between experiment and correlation with various wall orientation

4. Conclusions

In this study, the heat flux partitioning model was compared and validated with the experimental data of liquid-vapor phase, temperature and heat flux distributions on the wall and the bubble shape for nucleate boiling of saturated water at wall superheat of

7.5°C with various wall orientation of 0° (horizontal), 30°, 60°, 90° (vertical).

- The magnitude of the total wall heat flux was inconsistent between experiment and correlation. The heat flux prediction error larger than 50% was found for all the data from the various orientations. In addition, the prediction error increases as the boiling wall inclines from the horizontal to vertical.
- The prediction correlation for bubble parameters in the wall heat partitioning model was directly compared with the experimental results. The significant difference exists between the results measured from experiment and calculated with correlation.

ACKNOWLEDGEMENT

This work was supported by the Energy Efficiency & Resources of the Korea Institute of Energy Technology Evaluation and Planning (KETEP) grant funded by the Korea government Ministry of Knowledge Economy (No. 20131520000090)

REFERENCES

- [1] W. K. In, C. H. Shin, D. S. Oh, and T. H. Chun, Numerical Analysis of the Subcooled Boiling Flow in a Heated Rod Bundle, The Third National Congress on Fluids Engineering, August 26-28, Jeju, Korea 2004.
- [2] G. Son, Numerical Simulation of Bubble Motion during Nucleate Boiling, Trans. Korean Soc. Mech. Eng. B, Vol. 25, No. 3, pp. 389-396, 2001.
- [3] N. Kurul and M. Z. Podowski, Multidimensional Effects in Forced Convection Subcooled Boiling, Proceeding of the 9th Int. Heat Transfer Boiling, Vol. 2, pp. 19-24, 1990.
- [4] N. Basu, G. R. Warrier, and V. K. Dhir, Wall Heat Flux Partitioning during Subcooled Flow Boiling: Part I - Model Development, Journal of Heat Transfer, Vol. 127, pp. 131-140, 2005.
- [5] N. Basu, G. R. Warrier, V. K. Dhir, Wall Heat Wall Heat Flux Partitioning during Subcooled Flow Boiling: Part II - Model Validation, Journal of Heat Transfer, Vol. 127m pp. 141-148, 2005.
- [6] S. Jung and H. Kim, An experimental method to simultaneously measure the dynamics and heat transfer associated with a single bubble during nucleate boiling on a horizontal surface, Int. J. Heat and Mass Transfer, Vol. 73, pp. 365-375, 2014.
- [7] CUPID 1.8 Code Manual Volume 1: Mathematical Models and Solution Methods, Korea Atomic Energy Research Institute.